OMNIVIEWS

Omni-directional Visual System

IST-1999-29017

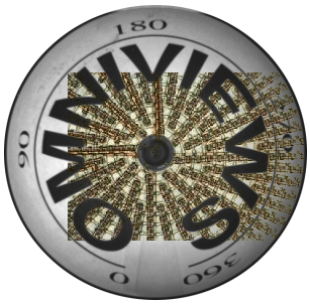

OMNIVIEWS Mirror Design and Software Tools

Cláudia Deccó, José Gaspar, Niall Winters, José Santos-Victor
Instituto Superior Técnico
Lisboa, Portugal
{ccgdecco,jag,niall,jasv}@isr.ist.utl.pt

September 2001

Contents

1 Introduction

This report describes the work done by Instituto Superior Técnico (IST) in the context of the IST-1999-29017 Project OMNIVIEWS from Sept. 1st 2000 - Sept. 1st 2001.

The work described in this report is mainly concerned with the design of the OMNIVIEWS mirror profile. The specifications arising from application to tracking and visual navigation have motivated the design of different mirror profiles matching each application needs. We have studied the theoretical models for the design of the mirror shape and developed a flexible software for mirror design according to various parameters. Based on the application of tracking and navigation a number of design parameters are considered when computing the mirror profile. Specific details on the applications based on these Omnivies cameras can be found in [5, 2].

In the framework of the Omniviews Project the fundamental idea is that of designing the mirror profile and the layout of the sensor in order to obtain geometric and computational benefits for the resulting image/processing.

Due to the rotational symmetry of the omnidirectional images, a natural choice is to use an image sensor with a polar structure. In this project we have used the SVAVISCA [6] log-polar sensor developed by DIST. As a result, panoramic images can be directly read out from the sensor with uniform angular resolution and without requiring any additional processing or image warping.

As the sensor radial pixel distribution is for the time being fixed (logarithm decay of resolution towards the periphery), the mirror profile provides the necessary degrees of freedom to modify the image geometry. In the Omniviews consortium, we have considered two image constraints:

- **Constant vertical resolution** - This design constraint aims to produce images, where objects at a (pre-specified) fixed distance from the camera's optical axis will always be the same size in the image, independent of its vertical coordinates. As a practical example this viewing geometry would allow for reading signs or text on the surfaces of objects with minimal distortion. As another example, tracking is facilitated by reducing the amount of distortion that an image target undergoes when an object is moving in 3D. Finally, in visual navigation it helps by providing a larger degree of invariance of image landmarks w.r.t the viewing geometry.

- **Constant horizontal resolution** - The constant horizontal resolution ensures that the ground plane is imaged under a scaled Euclidean transformation. As such, it greatly facilitates the measurement of distances and angles directly from the image as well as easier tracking of points lying on the pavement thus having a large impact on navigation algorithms.

The cross sections of these mirrors were obtained by projecting the rays of planes of the world in the image plane. Other constraints could be used such as ensuring uniform angular resolution as if the camera had a spherical geometry.

We have also designed a so-called *Mixed Mirror*, where the outer part of the image sensor is used to obtain a constant vertical resolution image, while the inner part is devoted to yield a constant horizontal resolution image. In this case, both the differential constraints on the mirror shape resulting from the two design goals are combined together in a single profile.

Even though the project will concentrate on polar pixel distributions we have also computed the corresponding mirror profiles when a standard (cartesian pixel distribution)camera is used.

1.1 Log-Polar Sensor

As previously stated, the rotational symmetry of the omnidirectional images immediately suggests the adequacy of using a polar pixel distribution. In the first phase of Omniviews we will use the SVAVISCA log-polar sensor, described in [6], charaterized by a log-polar pixel distribution. Hence, by using this image sensor coupled with an omnidirectional catadioptric camera, we will have two main advantages:

- Panoramic images can be directly read out from the sensor without the need for any geometric transformations.
- The panoramic image will have constant horizontal resolution due to the fact that the log-polar sensor is organized as concentric rings with a constant number of pixels.

In this section we briefly revise the characteristics of the SVAVISCA log-polar sensor for the sake of completeness of this report. The log polar sensor is shown in Figure 1.

Figure 1: General view of the SVAVISCA Log Polar Sensor (left). Detailed views of the foveal (center) and retinal (right) regions.

Inspired by the resolution of the human retina, the log-polar sensor is divided in two parts: the fovea and the retina. The fovea is the inner part of the sensor, with uniform pixel density and a radius of $\rho_0 = 0.027273cm$. Instead, the retina is the outer part of the sensor, consisting of a set of concentric circular rings, with a constant number of pixels, whose resolution decays logarithmically towards the image periphery. The sensor main specifications are summarized below:

- The fovea has 42 rings. The fovea has a constant pixel-size; the distribution of pixels is such that we have 1 pixel in the first ring, 6 in the second, an then 12, 18, 24, etc, until reaching the number of 252 pixels in the 42^{nd} ring;
- The retina has 110 rings, with 252 pixels each;
- The total number of pixels is 33.193 where 5.166 is in the fovea;
- The minimum size of pixel is $6.8 \times 6.45\mu m^2$;

- In the fovea the minimum pixel height is 6.52 μm;
- The fovea radius is $\rho_0 = 272.73 \mu m$;
- The increase rate of pixel in the retina is $k = 1.02337$;
- The diameter of sensor is $\rho_m ax = 7,135.44 \mu m$.

Hence, in the retinal part, the relation of the linear distance, ρ, measured on the sensor's surface and the corresponding pixel coordinate, p, is specified by:

$$p = \log_k(\rho/\rho_0) \tag{1}$$

where ρ_0 and k stand for the fovea radius and the rate of increase of pixel size towards the periphery.

2 Mirror Profile Design

Of course, each application for the Omniviews sensor may have different requirements. Our goal is to design a mirror profile to match the sensor's resolution in order to meet, in terms of desired image properties, a given application constraints.

The image formation process is determined by the trajectory of rays that start from a 3D point, reflect in the mirror surface and finally intersect with the image plane. This process depends on the projection function that specifies a type of sensor. Overall we want to shape the mapping between some world distances, y, and corresponding (pixel) distances measured in the image sensor. When considering constant resolution cameras pixel distances are obtained by scaling, ρ. For the case of constant resolution cameras there is a linear relation between sensor distances, ρ expressed in meters and the corresponding distance measured in pixels. Instead, for log-polar sensors this relation is logarithmic, expressed by Eq. (1). Hence, the design goal consists in meeting the following constraints:

$$y(\rho) = \begin{cases} a\rho + b, & \text{for a linear image sensor} \\ \\ a \log_k(\rho/\rho_0) + b, & \text{for the log polar sensor.} \end{cases}$$

for some values of a and b which mainly determine the visual field.

In the following sections, we will specify which 3D distances, $y(\rho)$, we want to map linearly to pixel coordinates, hence aiming to preserve different image invariants (e.g. ratios of distances or angles in certain directions).

2.1 Constant Vertical Resolution

Due to the rotational symmetry of the system we only need to consider the design of the mirror profile. The geometry of the image formation of the omnidirectional catadioptric camera is shown in Figure 2.

The first design procedure aims to preserve relative vertical distances of points placed at a fixed distance, d, from the camera's optical axis. In other words, if we consider a cylinder of radius, d, aligned with the camera optical axis, we want to ensure that ratios of distances measured in the

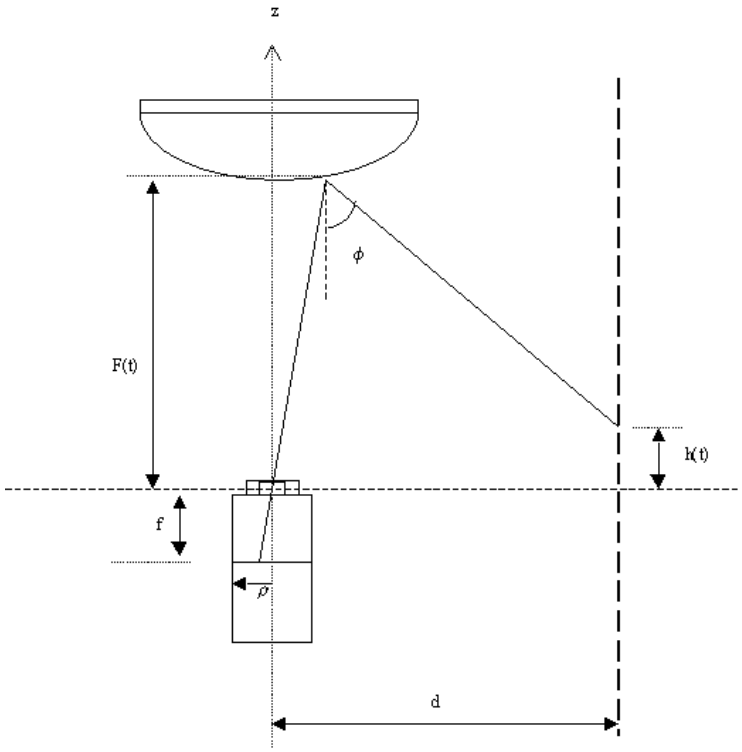

Figure 2: Projection of the rays of the vertical resolution

vertical direction along the surface of the cylinder would remain unchanged when measured in the image. Such invariance should be obtained by adequately designing the mirror profile - yielding a constant vertical resolution mirror.

The derivation described here follows closely that presented in [1]. The main differences consist of (i) a simpler setting for the equations describing the mirror profile and (ii) the analysis of numerical effects when computing the derivatives of the mirror-profile to build a quality index. We start by deriving a relationship between the elevation angle, ϕ, mirror profile, $F(t)$ and height, $h(t)$:

$$h(t) = F(t) - \cot(\phi)(d - t)$$

Equaling the angles of the incident and coincident rays in the mirror surface, we can relate $\cot(\phi)$ with the local slope, $F'(t)$, of the mirror profile, yielding:

$$h(t) = F(t) + \frac{2tF'(t) - F(t)(1 - F'(t)^2)}{2F(t)F'(t) + t(1 - F'(t)^2)}(d - t)$$

Solving this equation for $F'(t)$ we finally have:

$$F'(t) + \frac{t(d-t) + F(t)(F(t) - h(t))}{F(t)(d-t) - t(F(t) - h(t))} + \sqrt{\left[\frac{t(d-t) + F(t)(F(t) - h(t))}{F(t)(d-t) - t(F(t) - h(t))}\right]^2 + 1} = 0 \qquad (2)$$

We can now introduce the constraint that distances along the vertical direction, $h(t)$, should have an affine mapping with respect to radial pixel coordinates. Considering the different radial distribution

of pixels according to the cartesian or log-polar sensors, we have:

$$h(\rho) = \begin{cases} a\rho + b, & \text{for a linear image sensor} \\ \\ a \log_k(\rho/\rho_0) + b, & \text{for the log polar sensor.} \end{cases} \tag{3}$$

Finally, we can replace the sensor radial distances, ρ by mirror radial coordinates, t, by using the perspective projection equation:

$$\rho = \frac{f\, t}{F(t)} \tag{4}$$

Hence, the procedure to determine the mirror profile consists of integrating Eq. (2), while t varies from 0 to the mirror radius and replacing $h(t)$ by equations (3) and (4). The numerical integration was performed using MatLab's ode45 function.

The initialization of the integration process is done by computing the value of $F(0)$ that would allow the mirror rim to occupy the entire field of view of the sensor, while neglecting the thickness of the mirror shape (which is not available during initialization). From equation (4), we then have:

$$F(0) \approx \frac{f\, t_{max}}{\rho_{max}} \triangleq F_0 \tag{5}$$

where t_{max} and ρ_{max} represent the mirror and sensor radius, respectively.

We have not encountered problems due to this approximation. Should it be a problem in the future, one possible alternative would be to start the integration at the mirror rim and then proceed towards the center. Figure 3 show examples of mirror profiles for constant vertical resolution obtained for the linear and log-polar sensors.

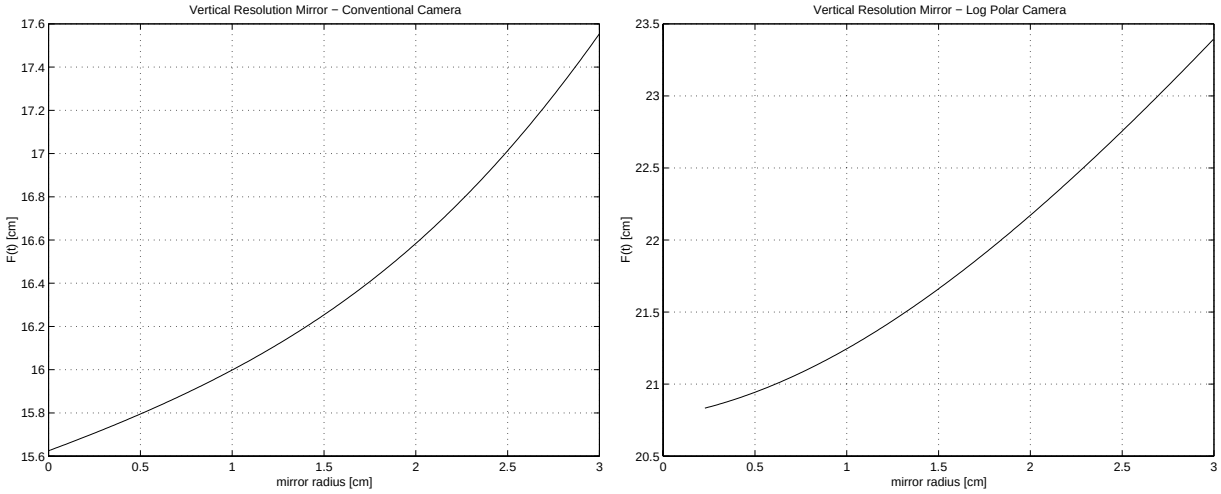

Figure 3: Constant vertical resolution mirrors for the conventional (left) and log-polar (right) image sensors.

2.2 Constant Horizontal Resolution (*Bird's Eye View*)

Another interesting design possibility for some applications is that of preserving ratios of distances measured on the ground plane. In such a case, one can directly use image measurements to obtain

ratios of distances or angles on the pavement (which can greatly facilitate navigation problems or visual tracking). Such images are also termed *Bird's eye views*. Figure 4 shows how the ground plane is projected onto the image plane, where the camera-to-ground distance is represented by h and $d(t)$ represents radial distances on the ground plane.

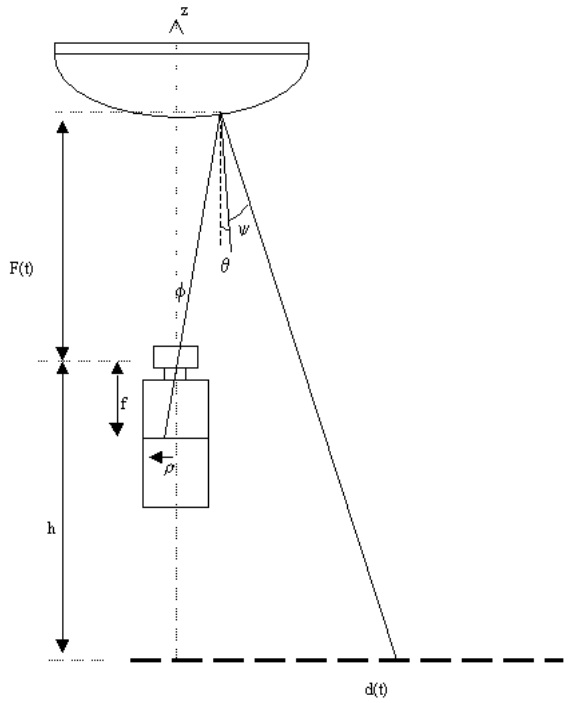

Figure 4: Projection of the rays of the horizontal resolution

Again, by equaling the incident and coincident angles, ϕ and $\Psi+\theta$ we note that $\Psi+\theta=\phi$, yielding:

$$tan(\phi+2\theta)=tan(\Psi+\theta)=\frac{d(t)-t}{F(t)+h}$$

where $F(t)$ denotes the distance to a mirror point measured from the optical center; t stands for the mirror radial distance. These angles can be expressed as a function of mirror profile, $F(t)$ and its local slope $F'(t)$, according to:

$$tan(2\theta)=\frac{2F'(t)}{1-F'(t)^2} \quad \text{and} \quad tan(\phi)=\frac{t}{F(t)},$$

Using these equations, we get:

$$d(t)=t+\frac{t(1-F'(t)^2)+2F(t)F'(t)}{F(t)(1-F'(t)^2)-2tF'(t)}(F(t)+h)$$

which can be solved for $F'(t)$, yielding:

$$F'(t)-\frac{t(d(t)-t)+(F(t)+h)F(t)}{(F(t)+h)t+(t-d(t))F(t)}-\sqrt{\left[\frac{t(d(t)-t)+(F(t)+h)F(t)}{(F(t)+h)t+(t-d(t))F(t))}\right]^2+1}=0 \qquad (6)$$

This equation expresses how the mirror shape determines which point on the ground plane, $d(t)$ is viewed at a specific mirror coordinate, t. As we did for the constant vertical-resolution mirror, we will now impose the constraint of an affine mapping between distances measured on the ground and those in the image. Taking into account the linear versus logarithmic pixel distribution, we will have:

$$d(\rho) = \begin{cases} a\rho + b, & \text{for a linear image sensor} \\ \\ a \log_k(\rho/\rho_0) + b, & \text{for the log polar sensor.} \end{cases} \tag{7}$$

The final step consists of expressing the radial distances measured in the sensor and the radial coordinate of the mirror, by means of the perspective projection:

$$\rho = \frac{f\, t}{F(t)} \tag{8}$$

The shape of the mirror profile, for constant horizontal resolution, is obtained by numerically integrating equation (6) subject to the constraints expressed by equations (8) and (7). Figure 5 shows examples of mirror profiles for constant horizontal resolution obtained for the linear and log-polar sensors.

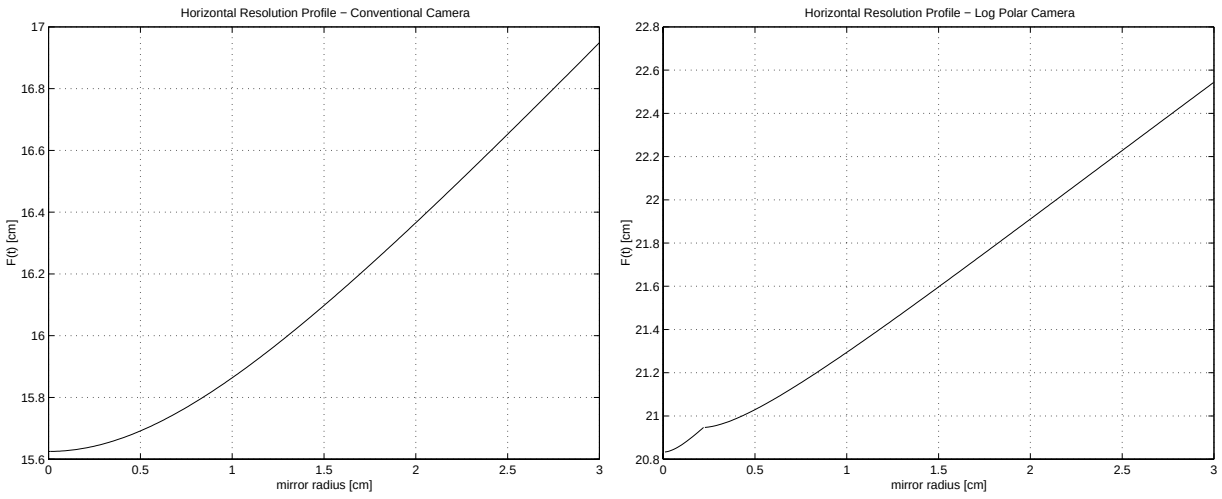

Figure 5: Constant horinzontal resolution mirrors for the conventional (left) and log-polar (right) image sensors.

2.3 Mixed Mirror

In some applications, one may be interested in having some type of mapping for a certain area of the visual field while some other area of the visual field is mapped in another way. This is typically the case for navigation where the constant vertical resolution mirror would facilitate tracking of vertical landmarks, while the *Bird's eye view* would make localization with respect to ground plane features easier.

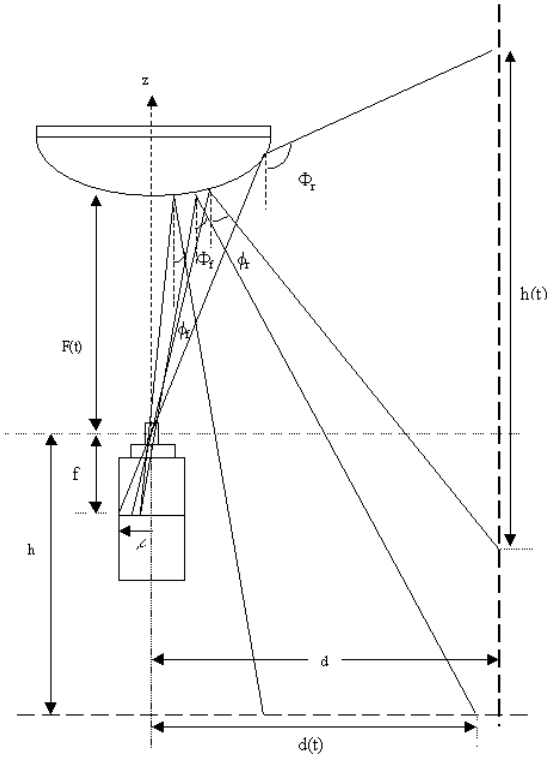

Figure 6: Viewing geometry of the mixed mirror.

Keeping this idea in mind we have considered a mixed mirror design where the inner part of the sensor is used for mapping the ground plane while the external part is used for representing the vertical structure. The geometry of such mirror is shown in Figure 6.

The field of view for each part of the sensor is determined by the corresponding parameters, a and b, which determine the vertical/horizontal segments that must be mapped onto the image.

We assume that the following input parameters are available:

$$\begin{cases} \phi_{f,r}/\Phi_{f,r} : \text{minimum/maximum view angles for the foveal/retinal region.} \\ t_{f,r} : \text{radius of the foveal/retinal mirror sections} \\ \rho_0 : \text{minimum radius of the log-polar sensor} \\ \rho_f : \text{radius of the “foveal” region of the sensor} \\ \rho_{max} : \text{radius of the image sensor} \\ d/D : \text{Minimum/maximum distances observed on the ground floor.} \\ h/H : \text{Minimum/maximum heights observed in the vertical direction.} \end{cases}$$

Using the geometry depicted in Figure 6, we can relate the desired fields of view specified by a user

and the corresponding minimum and maximum distances observed on the horizontal (to be mapped onto the fovea) and vertical directions (to be mapped by the retina).

In this case, by fovea we mean the inner part of the sensor and not necessarily the true *fovea* that can be found on the log-polar sensor. Hence the user also specifies the fraction of the mirror surface that should be used to map the horizontal/vertical directions.

From these specifications, we can determine the parameters a and b required for solving the problem. Table 1 indicates how to compute all the necessary parameters from the user input.

	FOVEA		**RETINA**	
	linear	*log-polar*	*linear*	*log-polar*
d	$\tan\phi_f(F_0+h)$		-	-
D	$t_f+\tan\Phi_f(F(t_f)+h)$ $\approx t_f+\tan\Phi_f(F_0+h)$		-	-
h			$\frac{d-t_f}{\tan\phi_r}-F(t_f)\approx\frac{d-t_f}{\tan\phi_r}-F_0$	
H			$\frac{d-t_r}{\tan\Phi_r}-F(t_r)\approx\frac{d-t_r}{\tan\Phi_r}-F_0$	
a	$\frac{D-d}{\rho_f}$	$\frac{D-d}{\log_k(\rho_f/\rho_0)}$	$\frac{H-h}{\rho_{max}-\rho_f}$	$\frac{H-h}{\log_k(\rho_{max}/\rho_f)}$
b	d	d	$h-a*\rho_f$	$h-a*\log_k(\rho_f/\rho_0)$

Table 1: Computation of the parameters a and b as a function of the observed distances or field of view.

Notice that as the mirror shape is not determined at this point we have to approximate the value of $F(t)$ by F_0 (see equation (5)) which may lead to slight changes in the obtained fields of view at the end of the whole procedure. In the future this design process can be improved by e.g re-iterating the mirror design and the process of computing a and b or by introducing these constraints directly when obtaining the differential equations that specify the mirror shape. Figure 7 show examples of mirror profiles for constant vertical resolution obtained for the linear and log-polar sensors. In this example we have used $\phi_f = 28^0$, $\Phi_f = 52^0$, $\phi_r = 80^0$, $\Phi_r = 115^0$ as the parameters determining the foveal and retinal fields of view. The camera height was defined as $h = 70cm$, the radius of the cylinder as $d = 200cm$ and the focal length used was $12.5cm$ and $25cm$ for the conventional/log-polar sensors. In all cases, the mirror diameter was set to $3cm$.

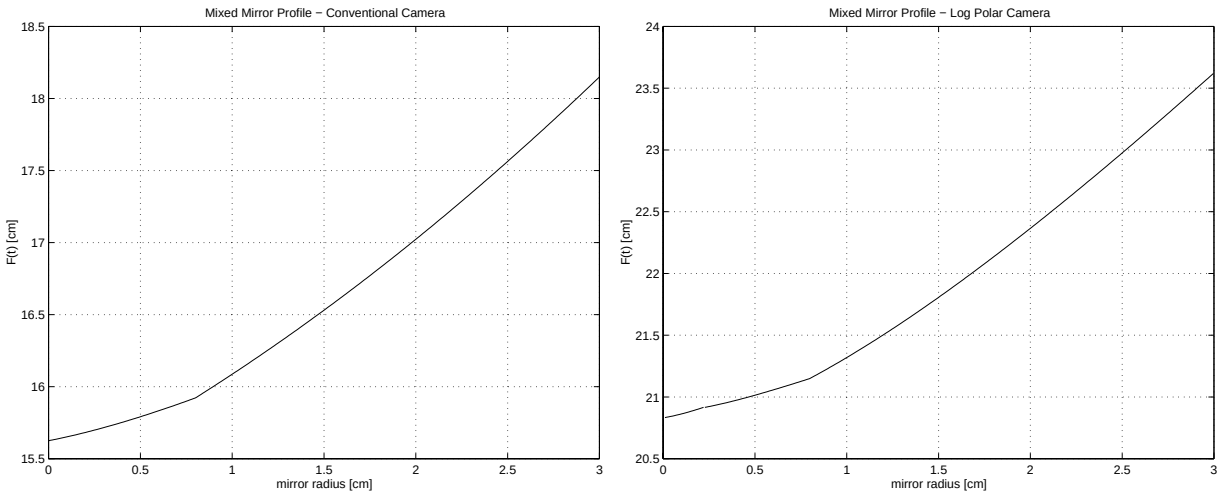

Figure 7: Mixed mirrors for both the conventional (left) and log-polar (right) image sensors. The parameters used for the foveal and retinal fields of view were $\phi_f = 28^0$, $\Phi_f = 52^0$, $\phi_r = 80^0$, $\Phi_r = 115^0$. The camera was placed $70cm$ above the ground and the radius of the cylinder was set as $d = 200cm$. The focal length used was $12.5cm$ and $25cm$ for the conventional/log-polar sensors. In all cases, the mirror diameter was set to $3cm$.

2.4 Analysis of the Mirrors and Results

In this section we analyze the quality of the obtained mirror profiles. There are two main factors whose influence is important to discuss:

- Numerical Errors - As we do not have an analytic description of the mirror shape and the actual profile is obtained through numerical integration it is important to verify the influence of numerical integration errors in the overall process.
- Sensitivity - As the Omniviews camera does not have a single center of projection, the linear mappings obtained between pixel distances and world distances is only valid for specific world surfaces (e.g. specific vertical cylinders or horizontal planes in our case). What happens if the radius of the cylinder is changed ?

Figure 8 shows how projection rays leading to uniform mappings at a certain distance will not have the same configuration for another distance.

As proposed in [1], the analysis of the mirror profile is done by calculating a quality index, $q(\rho)$. This quality index is defined as the ratio the between the numerical estimate of rate of the variation of the function $h(\rho)$ with respect to distances in the image plane, $[\partial h/\partial \rho]_n$, and the corresponding theoretical value, $[\partial h/\partial \rho]_t$.

$$q(\rho) = \frac{[dh(\rho)/d\rho]_n}{[dh(\rho)/d\rho]_t} \tag{9}$$

For the perfect design process we should have $q(\rho) = 1$. Computing $q(\rho)$ involves numerically differentiating the profile $F(t)$. Here we use different discrete approximations to derivatives as well as

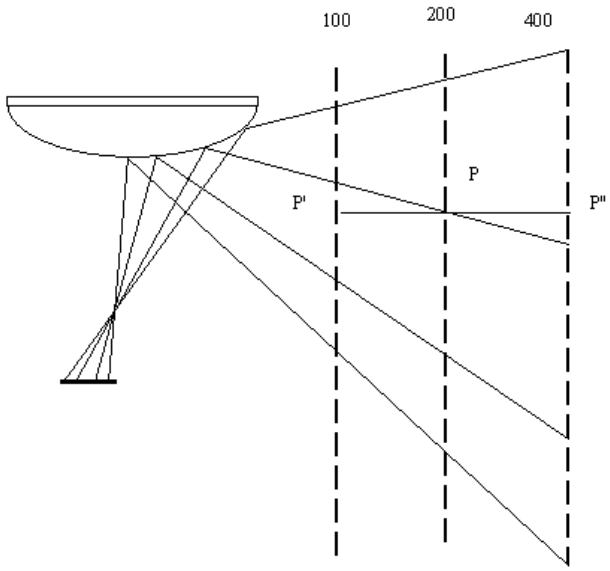

Figure 8: Projection of the rays in different distances

the theoretical expression for the mirror local slope. In the following figures we present some results obtained with different methods of derivations.

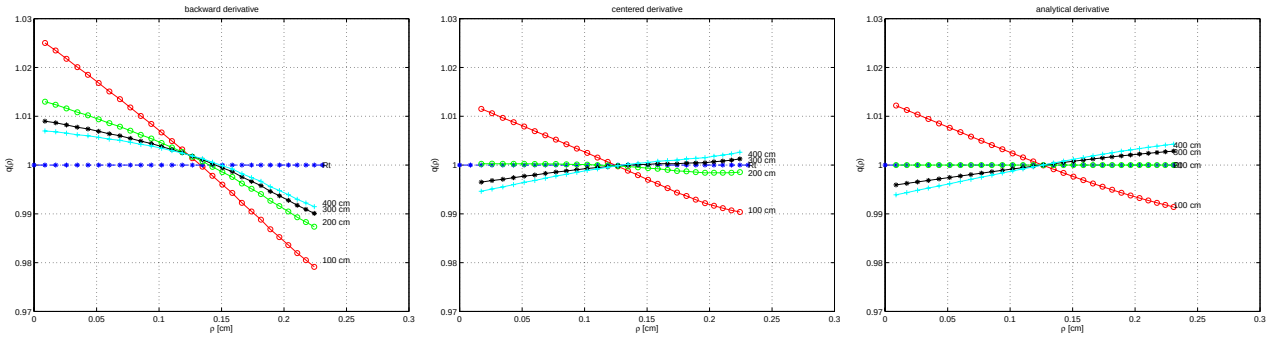

Figure 9: Analysis of the design criterion for different distances with a conventional image sensor using different numeric approximations to the derivative: backward (left) and centered (middle) differences versus the use of the analytic equation for $F'(t)$ (rightmost).

These results show two main aspects. Firstly, the influence of varying distance with respect to the desired mapping properties does not seem to be too important, which suggests that we are close to the situation of a single projection center. Secondly, the way derivatives are computed is very important in terms of quality analysis. This is even more evident for the log-polar sensor where increasing the sensor resolution towards the fovea imposes strong constraints on the way to compute derivatives of the mirror profile.

Nevertheless, the overall results show that the numerically computed profile meets the design specifications up to an error of about 1%. Variations when the distance changes from the nominal $d = 200cm$

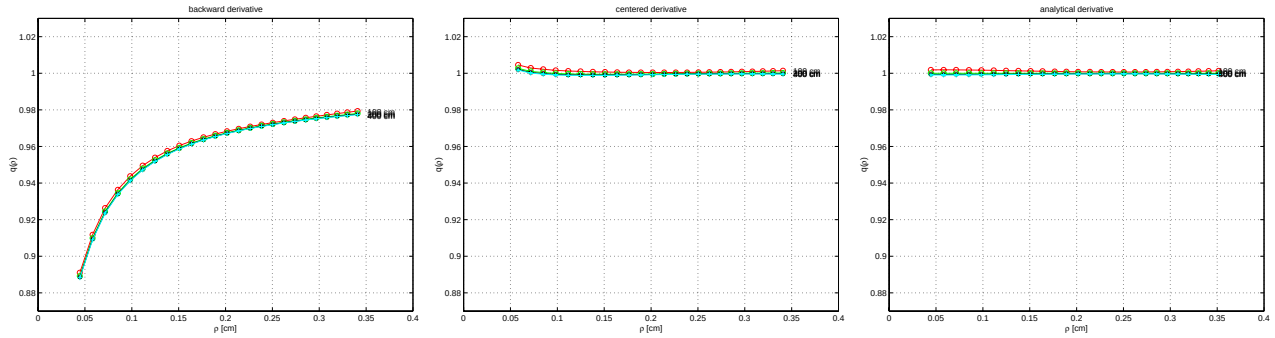

Figure 10: Analysis of the design criterion for different distances with a log-polar image sensor using different numeric approximations to the derivative: backward (left) and centered (middle) differences versus the usage of the analytic equation for $F'(t)$ (rightmost).

to $1m$ or $4m$ are not noticeable.

3 Software Description

We have developed a software tool to design the various types of mirrors described in this report. This software has been developed in MatLab and allows for designing a rich set of profiles simply by modifying the input parameters we have discussed in this report. In particular, we have defined a set of specifications in tune with the particular applications envisaged within the project.

The Graphical User Interface (gui) of Matlab is shown in Figure 11. We can visualize the mirror shapes for both cameras and the curves that allow us to analyze the curvature of the mirrors.

These mirrors will be projected by considering a linear relation between the position of the world point and the radial position of an image point.

4 Conclusions

In this report we have described a methodology to design and evaluate the profile or mirrors to be used in the Omniviews camera. The profile of the mirrors were designed according to the following specifications:

- Constant *vertical* resolution mirror - distances measured in a vertical line at a fixed distance from the camera axis, are mapped linearly to the image, hence eliminating any geometric distortion.
- Constant *horizontal* resolution mirror - where radial lines on the floor are mapped linearly in the image.
- Mixed mirror design - a single mirror combining distinct surfaces to provide constant vertical and horizontal resolution profiles.

We have shown how different specifications related to the desired visual fields can be translated in terms of the parameters leading to the mirror design.

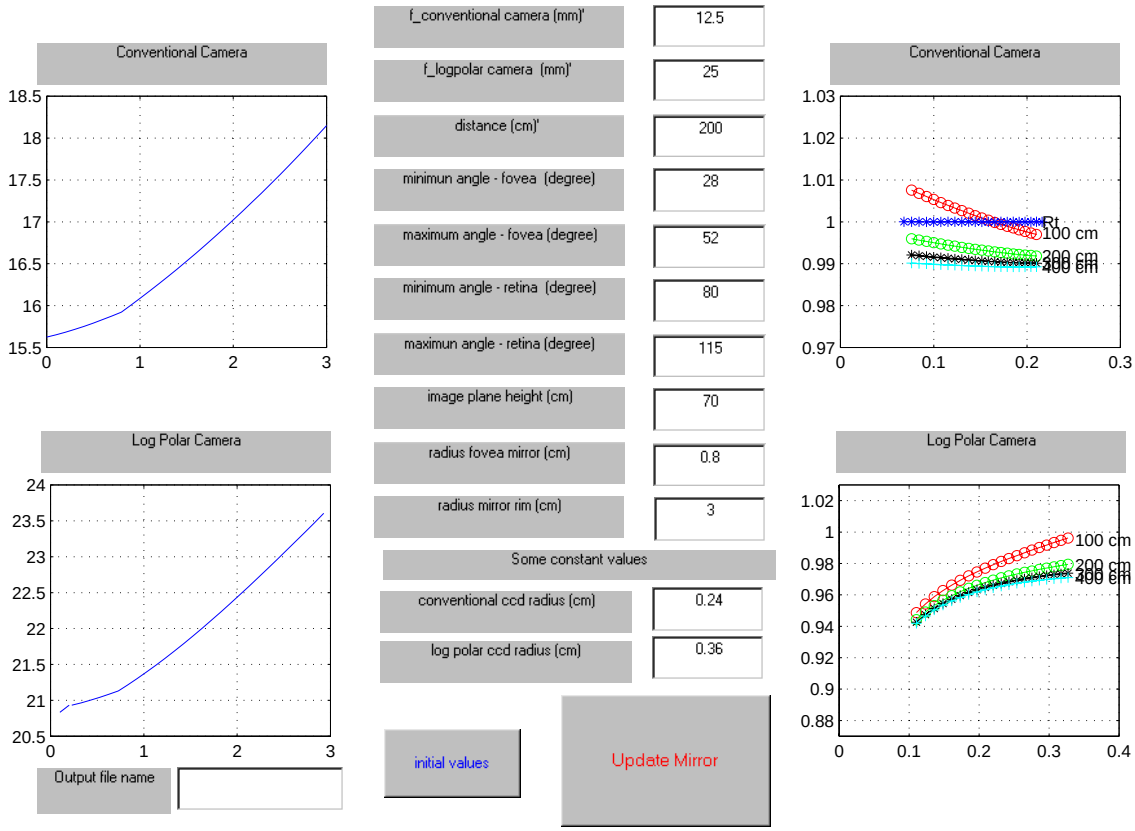

Figure 11: *Mirrordesign*: Interface of the application for mirror design.

We have also developed a flexible and powerful software tool that allows the user to vary all of the relevant input parameters.

A prototype of a mixed mirror has been built where the outer part of the sensor's retina is used for constant vertical resolution design; the inner part of the sensor's retina is used to generate the constant horizontal resolution criterion and the log-polar sensor's fovea has also been used, (in spite of the reduced number of pixels) to generate a bird's eye view of the ground floor.

References

[1] Gachter, Stefan; Pajdla, Tomás. "Mirror Design for an Omnidirectional Camera with a Uniform Cylindrical Projection when Using SVAVISCA Sensor" available at http://waltz.felk.cvut.cz/cmp/omniviews/.

[2] Gaspar, José; Winters, Niall and Santos-Victor, José. "Vision-based Navigation and Environmental Representations with an Omnidirectional Camera," *IEEE Transaction on Robotics and Automation,* Vol 16, 6, Dec. 2000.

[3] Hicks, R. A.; Bajcsy, R. "Refletive Surfaces as Computational Sensors", *Workshop on Perception for Mobile Agents at CVPR'99*, p. 82-86, Colorado, USA, June 1999;
(http://www.cs.yorku.ca/ jenkin/wpma2/pdf/hicks.pdf)

[4] Hicks, R.A.; Bajcsy, R.. "Catadioptric Sensors that Approximate Wide-angle Perspective Projections", *IEEE Workshop on Omnidirectional Vision - OMNIVIS'00* p: 97-103, June 2000.

[5] Winters, Niall; Gaspar, José; Bernardino, Alexandre and Santos-Victor, José. "Vision algorithms for Omniviews Cameras", Omniviews deliverable DI-3.

[6] "Document on Specification "- Esprit Project n. 31951 - SVAVISCA - available at http://www.lira.dist.unige.it - SVAVISCA - GIOTTO Home Page - 18/05/99.